

Supplementary Information

Rational molecular design of multifunctional self-assembled monolayers for efficient hole selection and buried interface passivation in inverted perovskite solar cells

Wenlin Jiang,^{†abc} Ming Liu,^{†ac} Yanxun Li,^{ac} Francis R. Lin,^{bc} and Alex K.-Y. Jen^{*abcd}

^a *Department of Materials Science and Engineering, City University of Hong Kong, Kowloon 999077 (Hong Kong) E-mail: alexjen@cityu.edu.hk*

^b *Department of Chemistry, City University of Hong Kong, Kowloon 999077 (Hong Kong)*

^c *Hong Kong Institute for Clean Energy, City University of Hong Kong, Kowloon 999077 (Hong Kong)*

^d *State Key Laboratory of Marine Pollution, City University of Hong Kong, Kowloon, 999077 (Hong Kong)*

[†]*These authors contributed equally to this work.*

Table of Contents

1. Materials and characterization techniques	3
2. Synthesis and characterization	4
3. Optical and Electrochemical Characterizations	7
4. Density Functional Theory (DFT) Calculation	8
5. Single crystal X-ray diffraction analysis.....	10
6. Surface Characterizations.....	11
7. Device Fabrication and characterization.....	15
8. ^1H and ^{13}C NMR spectra	17
9. References	24

1. Materials and characterization techniques

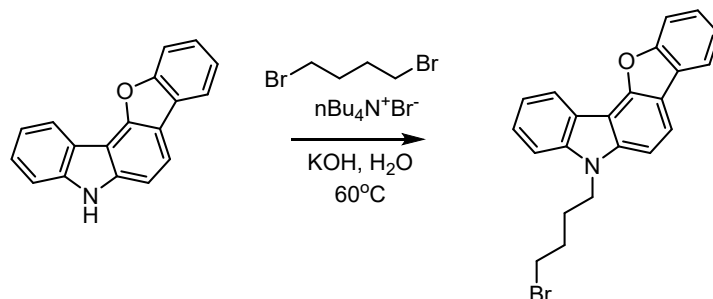
The reagents and starting materials were commercially available and used without any further purification, if not specified, 5*H*-Benzofuro[3,2-*c*]carbazole, and 5*H*-Benzo[4,5]thieno[3,2-*c*]carbazole are purchased from Bidepharm. CsI/C₆₀/BCP/MAI are purchased from Xi'an P-OLED. FAI is purchased from Solarmer. PbI₂ is obtained from TCI. DMF, DMSO, IPA, and CB are purchased from J&K. Compound **CbzPh** was synthesized according previous report.^[1]

¹H NMR and ¹³C NMR spectra were measured on Bruker AVANCE III 300MHz and 400MHz spectrometers. Matrix assisted laser desorption/ionization time-of-flight (MALDI-TOF) mass spectra were collected on a Bruker Solarix-XR high-resolution mass spectrometer (HR-MS). Single crystals used for X-ray diffraction analysis were obtained by slow evaporation in acetone. The data for the single crystals of 5*H*-Benzofuro[3,2-*c*]carbazole, and 5*H*-Benzo[4,5]thieno[3,2-*c*]carbazole were collected with a Rigaku Saturn diffractometer with CCD area detector. Crystallographic data (excluding structure factors) reported in this paper were deposited in the Cambridge Crystallographic Data Centre (CCDC No. 2298041 for 5*H*-Benzofuro[3,2-*c*]carbazole, CCDC No. 2298042 for 5*H*-Benzo[4,5]thieno[3,2-*c*]carbazole). Crystallographic data (excluding structure factors) of 7*H*-benzo[*c*]carbazole was deposited in the Cambridge Crystallographic Data Centre (CCDC No. 1412957).

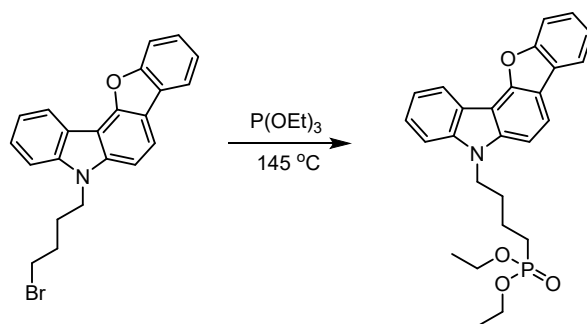
Solution and thin-film UV-Vis absorption spectra were obtained from Agilent8454 spectrophotometer. All film samples were spin-cast on ITO substrates. Solution UV-Vis absorption spectra were collected from the isopropanol solution of four SAMs with the concentration of 1.0×10^{-5} M. Cyclic voltammetry (CV) measurements were conducted on a CHI660D electrochemical workstation. The CV experiments were performed at room temperature with a conventional three-electrode system using a glassy carbon electrode as working electrode, Pt wire as the counter electrode, and an Ag/AgCl (saturated KCl) as the reference electrode. Tetrabutylammonium phosphorus hexafluoride (Bu₄NPF₆, 0.1M) in acetonitrile solution was used as the supporting electrolyte, and the scan rate was 0.1 Vs⁻¹. For calibration, the redox potential of ferrocene/ferrocenium (Fc/Fc⁺) was measured under the same condition. The SAMs were drop-cast onto the glassy carbon electrode from isopropanol solutions (1 mg mL⁻¹) to form thin films. HOMO energies of SAMs were estimated with the following equation: HOMO = $-(E_{\text{ox}}^{\text{onset}} + 4.8)$ eV. LUMO energies were estimated with the following equation: LUMO = (HOMO + $E_{\text{g}}^{\text{opt}}$) eV. UPS and XPS characterization are conducted in a VG ESCALAB 220i-XL surface analysis system equipped with a He discharge lamp ($h\nu = 21.22$ eV) and a monochromatic Al-K α X-ray gun ($h\nu = 1486.6$ eV). The samples are deposited on ITO in the same process as device fabrication. Typically, the characterized peak of hydrocarbon C1s from adventitious carbon at 284.8 eV is used for binding energy calibration. Surface potential of SAM modified ITO by Kelvin probe force microscopy (KPFM) was determined using Bruker 'MultiMode 8' Atomic Force Microscope (AFM) System and the probe is SCM-PIT-V2 (Pt-Ir coating on the front side) with the tip radius of 25 nm. Contact angle is measured with a DataPhysics contact angle tester and the water drop volume is set as 1 μ L. Surface morphology of perovskite films are characterized by scanning electron microscopy (SEM, Philips XL30

FEG). The XRD patterns for perovskite film crystallization analysis are measured by an X-ray diffraction (XRD) using a Bruker D2 Phaser with Cu K α radiation.

2. Synthesis and characterization

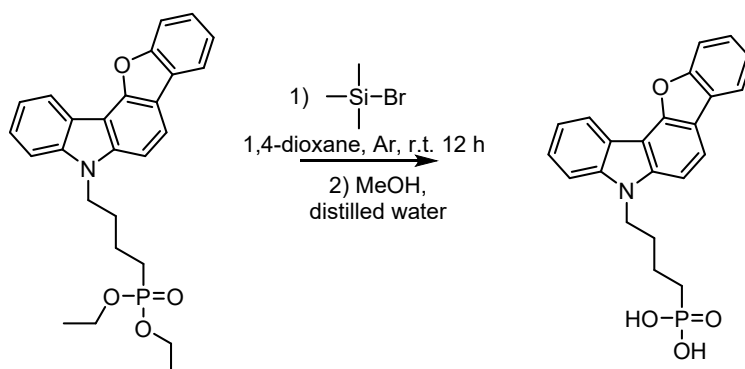


5-(4-bromobutyl)-5H-benzofuro[3,2-c]carbazole: 5H-benzofuro[3,2-c]carbazole (1 g, 3.89 mmol) was dissolved in 1,4- dibromobutane (20 eq, 15.69 g, 8.7 mL, 77.7 mmol), tetrabutylammonium bromide (0.15 eq, 0.188 g, 0.58 mmol) and 50% KOH aqueous solution (5 eq) were added subsequently. Reaction was stirred at 60 °C overnight. After completion of the reaction, extraction was done with dichloromethane. The organic layer was dried over anhydrous Na₂SO₄ and the solvent was distilled off under reduced pressure. The crude product was purified by column chromatography (*n*-hexane: dichloromethane 4:1 *v:v*) to give 1.43 g (93.8 %) of white powder. ¹H NMR (300 MHz, Chloroform-*d*) δ 8.54 (d, *J* = 7.8 Hz, 1H), 8.04 – 7.94 (m, 2H), 7.73 (dd, *J* = 7.7, 1.4 Hz, 1H), 7.58 – 7.35 (m, 6H), 4.43 (t, *J* = 6.9 Hz, 2H), 3.39 (t, *J* = 6.4 Hz, 2H), 2.21 – 2.03 (m, 2H), 2.00 – 1.86 (m, 2H). ¹³C NMR (75 MHz, Chloroform-*d*) δ 156.17, 151.41, 140.80, 139.82, 125.56, 125.18, 122.89, 122.86, 120.61, 119.80, 119.61, 117.86, 115.79, 111.67, 108.68, 108.13, 104.35, 42.73, 33.16, 30.21, 27.76.

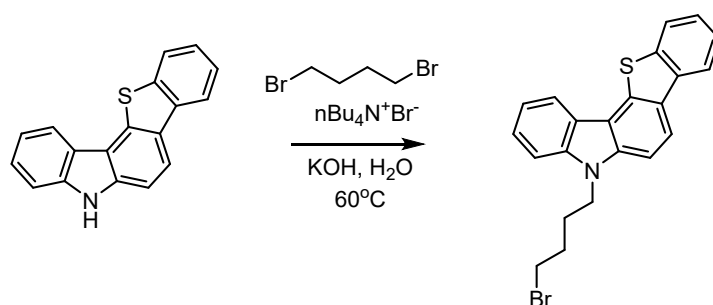


Diethyl (4-(5H-benzofuro[3,2-c]carbazol-5-yl)butyl)phosphonate: 5-(4-bromobutyl)-5H-benzofuro[3,2-c]carbazole (1.33 g, 3.39 mmol) was dissolved in triethyl phosphite (20 eq, 11.27 g, 11.63 mL, 67.8 mmol) and the reaction mixture was heated at 145 °C overnight. After reaction completion the solvent was distilled off under reduced pressure. The crude product was purified by column chromatography (dichloromethane:ethyl acetate 3:1 *v:v*) to give 1.40 g (92 %) of colorless oil. ¹H NMR (300 MHz, Chloroform-*d*) δ 8.52 (dt, *J* = 7.8, 1.0 Hz, 1H), 8.04 – 7.93 (m, 2H), 7.72 (dd, *J* = 7.4, 1.3 Hz, 1H), 7.57 – 7.33 (m, 6H), 4.42 (t, *J* = 7.1 Hz, 2H), 4.02 (qdd, *J* = 7.9, 5.7, 2.0 Hz, 4H), 2.10 – 1.98 (m, 2H), 1.75 (td, *J* = 7.0, 6.3, 3.1 Hz, 4H), 1.24 (t, *J* = 7.0

Hz, 6H). ^{13}C NMR (75 MHz, Chloroform-*d*) δ 156.14, 151.40, 140.83, 139.84, 125.50, 125.19, 125.13, 122.83, 120.57, 119.73, 119.58, 117.79, 115.70, 111.64, 108.71, 108.07, 104.40, 61.64, 61.55, 43.10, 29.95, 29.74, 26.36, 24.49, 20.49, 20.43, 16.47, 16.39.

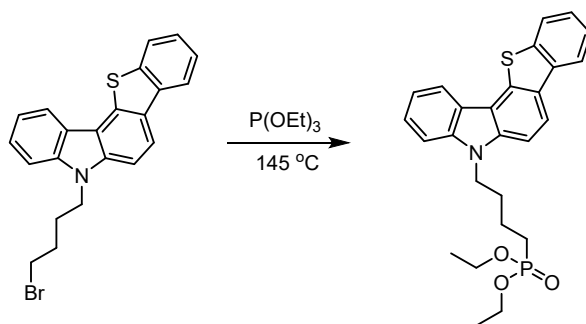


(4-(5H-benzofuro[3,2-c]carbazol-5-yl)butyl)phosphonic acid (CbzBF): Diethyl (4-(5H-benzofuro[3,2-c]carbazol-5-yl)butyl)phosphonate (1 g, 2.22 mmol) was dissolved in anhydrous 1,4-dioxane (22 mL) under argon atmosphere and bromotrimethylsilane (10 eq, 3.4 g 2.93 mL, 22.2 mmol) was added dropwise. Reaction was stirred for 12 h at room temperature under argon atmosphere. Afterwards solvent was partially distilled off under reduced pressure, and the liquid residue was dissolved in methanol (8 ml). Next, distilled water was added dropwise (40 ml), until solution became opaque. Product was filtered off and washed with water to give 0.72 g (82.3 %) of off-white solid. ^1H NMR (400 MHz, DMSO-*d*₆) δ 8.35 (d, $J = 7.7$ Hz, 1H), 8.20 – 8.11 (m, 2H), 7.82 (d, $J = 7.9$ Hz, 1H), 7.73 (dd, $J = 18.0, 8.4$ Hz, 2H), 7.54 (t, $J = 7.7$ Hz, 1H), 7.50 – 7.38 (m, 2H), 7.35 (t, $J = 7.4$ Hz, 1H), 4.52 (t, $J = 7.1$ Hz, 2H), 1.91 (p, $J = 7.0$ Hz, 2H), 1.58 (d, $J = 9.6$ Hz, 4H). ^{13}C NMR (100 MHz, DMSO-*d*₆) δ 155.77, 150.78, 141.10, 140.08, 126.14, 125.92, 125.13, 123.71, 122.21, 120.47, 120.15, 119.78, 118.74, 115.28, 112.04, 110.33, 107.26, 106.21, 43.12, 30.23, 30.08, 28.49, 27.13, 20.94, 20.89. HR-MS (MALDI-TOF): calcd. for $\text{C}_{22}\text{H}_{20}\text{NO}_4\text{P}$ [M]⁺ 393.1130; Found: 393.1130.

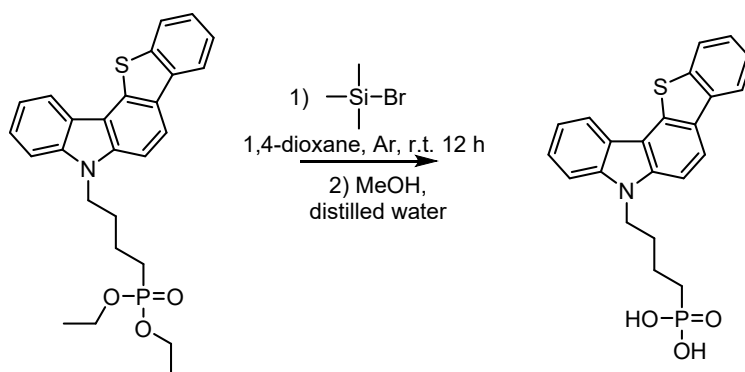


5-(4-bromobutyl)-5H-benzo[4,5]thieno[3,2-c]carbazole: 5H-benzo[4,5]thieno[3,2-c]carbazole (1 g, 3.66 mmol) was dissolved in 1,4- dibromobutane (20 eq, 14.77 g, 8.2 ml, 73.6 mmol), tetrabutylammonium bromide (0.15 eq, 0.55 mmol, 0.177 g) and 50% KOH aqueous solution (5 eq) were added subsequently. Reaction was stirred at 60°C overnight. After completion of the reaction, extraction was done with dichloromethane. The organic layer was dried over anhydrous Na_2SO_4 and the solvent was distilled off under reduced pressure. The crude

product was purified by column chromatography (*n*-hexane: dichloromethane 4:1 *v:v*) to give 1.42 g (95 %) of white powder. ¹H NMR (400 MHz, Chloroform-*d*) δ 8.27 (dt, *J* = 7.8, 1.0 Hz, 1H), 8.24 – 8.16 (m, 2H), 8.02 – 7.93 (m, 1H), 7.57 – 7.39 (m, 6H), 4.43 (t, *J* = 7.0 Hz, 2H), 3.37 (t, *J* = 6.5 Hz, 2H), 2.18 – 2.01 (m, 2H), 1.92 (ddd, *J* = 13.1, 9.0, 6.2 Hz, 2H). ¹³C NMR (100 MHz, Chloroform-*d*) δ 139.98, 139.31, 138.59, 136.08, 133.07, 128.27, 125.51, 125.19, 124.61, 123.00, 122.10, 121.81, 120.81, 119.76, 119.14, 116.53, 108.82, 106.43, 42.59, 33.12, 30.19, 27.83.



Diethyl (4-(5H-benzo[4,5]thieno[3,2-c]carbazol-5-yl)butyl)phosphonate: 5-(4-bromobutyl)-5H-benzo[4,5]thieno[3,2-c]carbazole (1.3 g, 3.18 mmol) was dissolved in triethyl phosphite (20 eq, 10.58 g, 10.92 mL, 63.67 mmol) and the reaction mixture was heated at 145 °C overnight. After reaction completion the solvent was distilled off under reduced pressure. The crude product was purified by column chromatography (dichloromethane:ethyl acetate 3:1 *v:v*) to give 1.35 g (91 %) of colorless oil. ¹H NMR (400 MHz, Chloroform-*d*) δ 8.31 – 8.15 (m, 3H), 8.00 – 7.93 (m, 1H), 7.57 – 7.47 (m, 4H), 7.47 – 7.36 (m, 2H), 4.43 (t, *J* = 7.1 Hz, 2H), 4.07 – 3.95 (m, 4H), 2.05 (p, *J* = 7.2 Hz, 2H), 1.78 – 1.68 (m, 4H), 1.23 (t, *J* = 7.1 Hz, 6H). ¹³C NMR (100 MHz, Chloroform-*d*) δ 140.02, 139.36, 138.58, 136.10, 133.06, 128.23, 125.46, 125.15, 124.59, 122.99, 122.08, 121.77, 120.79, 119.69, 119.10, 116.51, 108.85, 106.49, 61.59, 61.53, 43.01, 30.01, 29.85, 26.16, 24.75, 20.51, 20.46, 16.45, 16.39.



(4-(5H-benzo[4,5]thieno[3,2-c]carbazol-5-yl)butyl)phosphonic acid (CbzBT): Diethyl (4-(5H-benzo[4,5]thieno[3,2-c]carbazol-5-yl)butyl)phosphonate (1.13 g, 2.43 mmol) was dissolved in anhydrous 1,4-dioxane (24 ml) under argon atmosphere and bromotrimethylsilane (10 eq, 3.71 g 3.2 mL, 24.3 mmol) was added dropwise. Reaction was stirred for 12 h at room temperature

under argon atmosphere. Afterwards solvent was partially distilled off under reduced pressure, and the liquid residue was dissolved in methanol (8 ml). Next, distilled water was added dropwise (40 ml), until solution became opaque. Product was filtered off and washed with water to give 0.805 g (81 %) of white solid. ^1H NMR (400 MHz, $\text{DMSO-}d_6$) δ 8.45 – 8.36 (m, 2H), 8.15 – 8.08 (m, 2H), 7.84 (d, $J = 8.7$ Hz, 1H), 7.78 (d, $J = 8.2$ Hz, 1H), 7.60 – 7.44 (m, 3H), 7.39 (t, $J = 7.4$ Hz, 1H), 4.54 (t, $J = 7.0$ Hz, 2H), 1.91 (p, $J = 7.0$ Hz, 2H), 1.58 (t, $J = 7.9$ Hz, 4H). ^{13}C NMR (100 MHz, $\text{DMSO-}d_6$) δ 140.22, 139.67, 137.88, 136.19, 131.98, 128.00, 126.10, 125.90, 125.46, 123.66, 121.68, 121.35, 121.19, 120.15, 120.08, 115.68, 110.45, 108.24, 42.99, 30.32, 30.17, 28.49, 27.13, 20.94, 20.90. HR-MS (MALDI-TOF): calcd. for $\text{C}_{22}\text{H}_{20}\text{NO}_3\text{PS}$ $[\text{M}]^+$ 409.0902; Found: 409.0902.

3. Optical and Electrochemical Characterizations

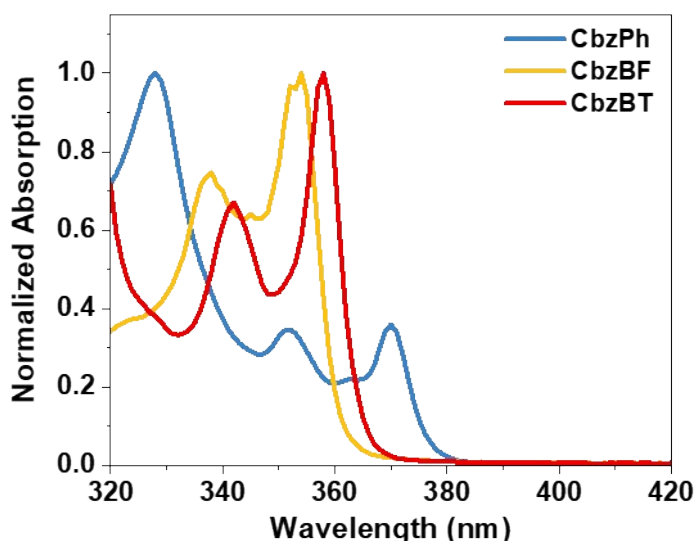


Figure S1. UV/Vis absorption spectra of CbzPh, CbzBF and CbzBT in solutions (10^{-5} M in IPA).

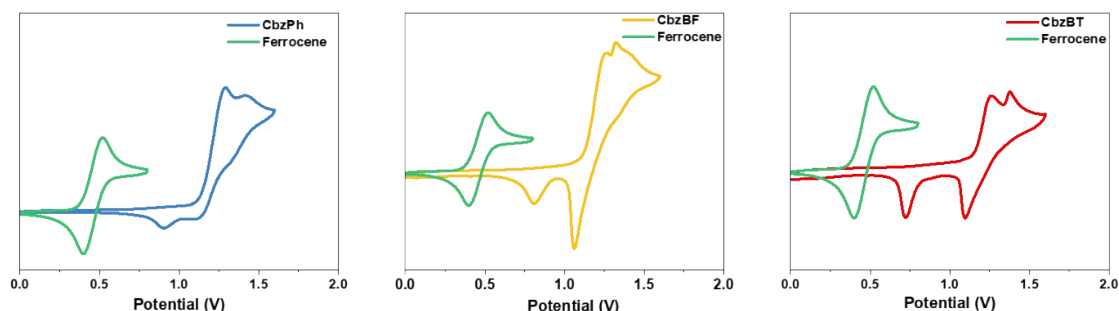


Figure S2. Cyclic voltammetry characterized oxidation potential of phosphates (see synthesis

section) corresponding to CbzPh, CbzBF and CbzBT in (1×10^{-3} M) in DCM with 0.1M Bu_4NPF_6 as electrolyte, glassy carbon and platinum wire as working and counter electrodes and Ag/AgCl as reference electrode; scanning rate was 100 mV/s; Ferrocene was used as external reference and the potentials were presented by reference to $E_{1/2}(\text{Fc}/\text{Fc}^+)$.

4. Density Functional Theory (DFT) Calculation

Computational Details: Geometries optimization and frequency analysis were performed at the level of B3LYP /6-311G(d,p). The molecular orbitals and dipole moments were analyzed, the energy gaps between HOMO and LUMO were obtained. All calculations are based on Density Functional Theory (DFT) with Gaussian09 package.^[2]

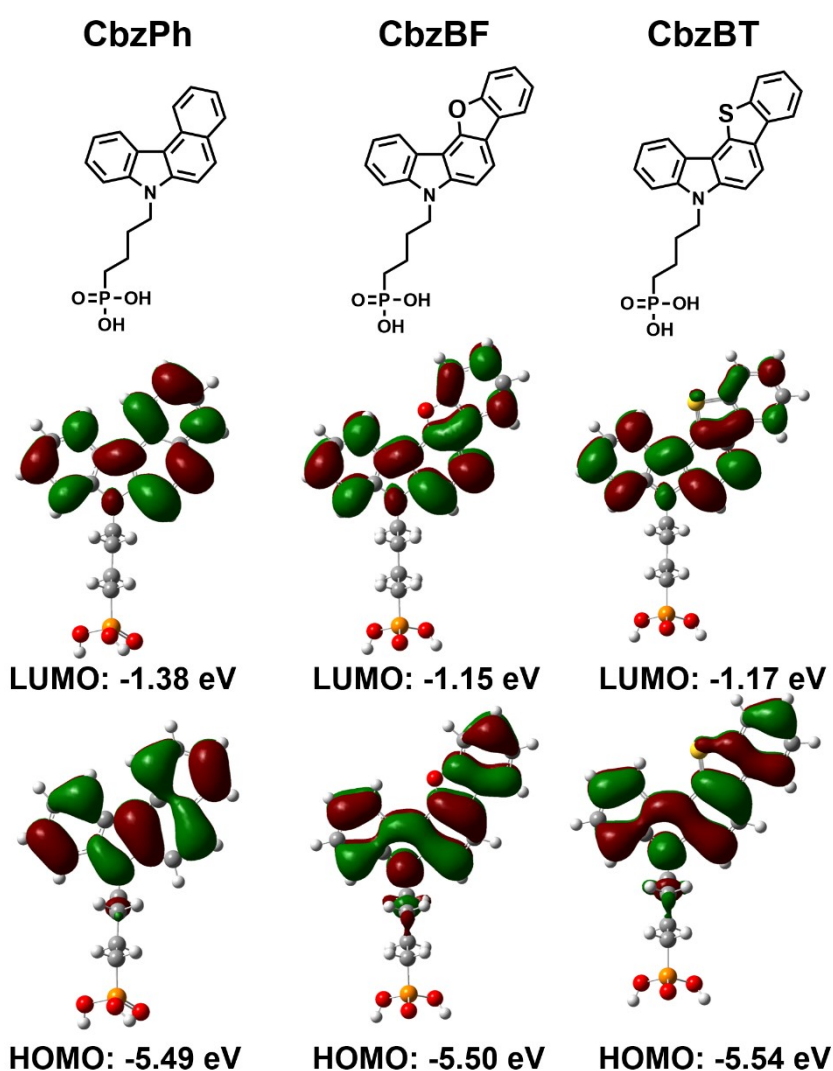


Figure S3. The calculated HOMO/LUMO orbitals and energy levels of CbzPh, CbzBF and CbzBT.

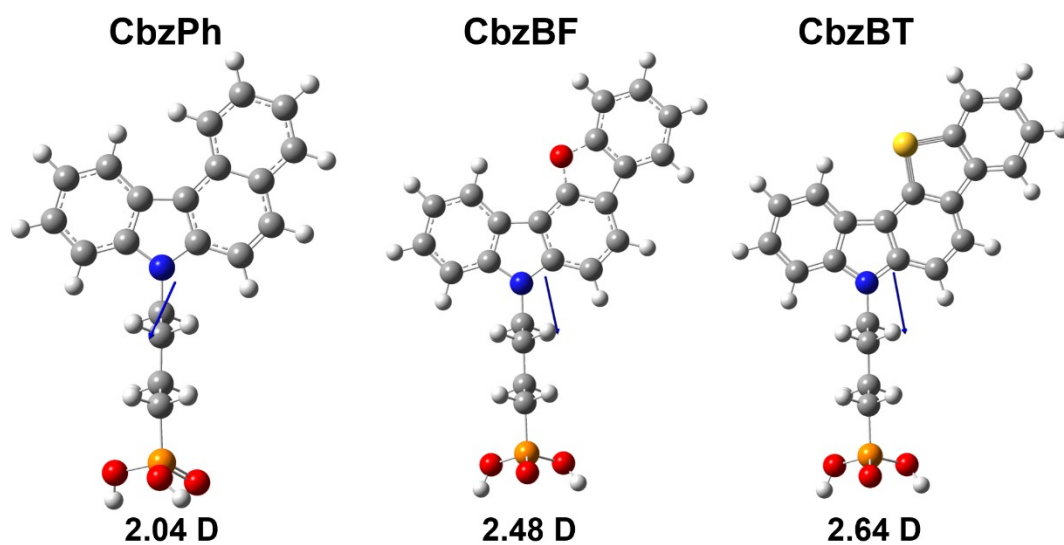


Figure S4. The calculated molecular structures and dipoles of CbzPh, CbzBF and CbzBT.

Table S1. Experimentally measured and theoretically calculated energy levels of CbzPh, CbzBF and CbzBT.

	Experimental			Optical band gap (eV)	Calculated	
	HOMO (eV) CV	HOMO (eV) UPS	LUMO (eV)		HOMO (eV)	LUMO (eV)
CbzPh	-5.48	-5.40	-2.19	3.29	-5.49	-1.38
CbzBF,	-5.46	-5.44	-2.02	3.44	-5.50	-1.15
CbzBT	-5.50	-5.45	-2.10	3.40	-5.54	-1.17

Optical band gaps obtained from the absorption edge of UV-Vis spectra.

5. Single crystal X-ray diffraction analysis

Table S2. Crystal data and structural refinement for 5*H*-Benzofuro[3,2-*c*]carbazole and 5*H*-Benzo[4,5]thieno[3,2-*c*]carbazole.

Identification code	070723a_wenlin	070723b_wenlin
CCDC deposition No.	2298041	2298042
Empirical formula	C ₁₈ H ₁₁ NO	C ₁₈ H ₁₁ NS
Formula weight	257.28	273.34
Temperature/K	193(2)	193(2)
Crystal system	monoclinic	orthorhombic
Space group	C2/c	Pna2 ₁
a/Å	21.6821(11)	15.7172(3)
b/Å	5.3270(4)	5.28910(10)
c/Å	22.9919(15)	31.0413(7)
α/°	90	90
β/°	114.126(5)	90
γ/°	90	90
Volume/Å ³	2423.6(3)	2580.46(9)
Z	8	8
ρ _{calc} /g/cm ³	1.410	1.407
μ/mm ⁻¹	0.694	2.098
F(000)	1072.0	1136.0
Crystal size/mm ³	0.22 × 0.11 × 0.02	0.31 × 0.08 × 0.03
Radiation	CuKα (λ = 1.54178)	CuKα (λ = 1.54178)
2θ range for data collection/°	8.938 to 148.95	5.694 to 149.212
Index ranges	-26 ≤ h ≤ 26, -6 ≤ k ≤ 6, -28 ≤ l ≤ 28	-19 ≤ h ≤ 19, -6 ≤ k ≤ 5, -38 ≤ l ≤ 38
Reflections collected	9881	21616
Independent reflections	2451 [R _{int} = 0.0456, R _{sigma} = 0.0396]	4942 [R _{int} = 0.0687, R _{sigma} = 0.0576]
Data/restraints/parameters	2451/0/181	4942/1/361
Goodness-of-fit on F ²	1.068	1.066
Final R indexes [I ≥ 2σ (I)]	R ₁ = 0.0384, wR ₂ = 0.1037	R ₁ = 0.0509, wR ₂ = 0.1378
Final R indexes [all data]	R ₁ = 0.0407, wR ₂ = 0.1064	R ₁ = 0.0574, wR ₂ = 0.1458
Largest diff. peak/hole / e ⁻ Å ⁻³	0.20/-0.23	0.22/-0.56

6. Surface Characterizations

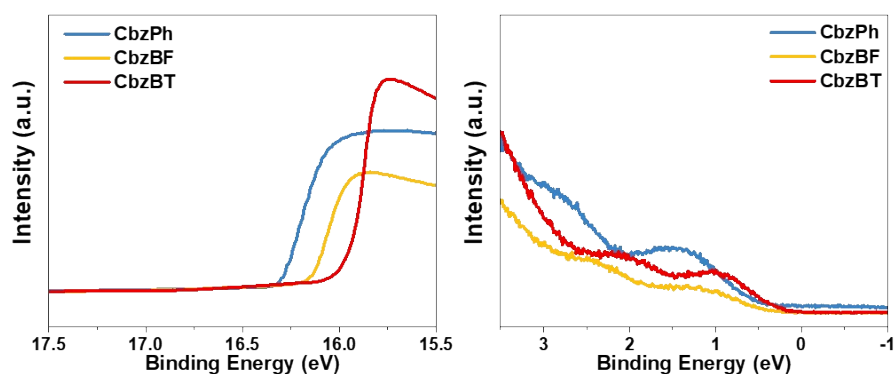


Figure S5. UPS spectra (using the He I lamp with a photon energy of 21.22 eV) of CbzPh, CbzBF and CbzBT modified ITO.

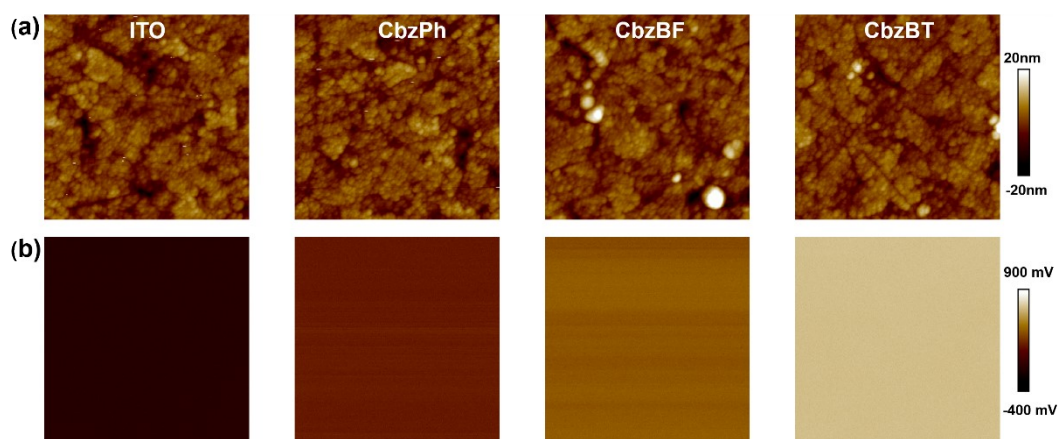


Figure S6. Surface potential profiles of CbzPh-, CbzBF- and CbBT-modified ITO substrates. (a) KPFM topography map and (b) surface contact potential difference (CPD) map of CbzPh-, CbzBF- and CbBT-modified ITO substrates.

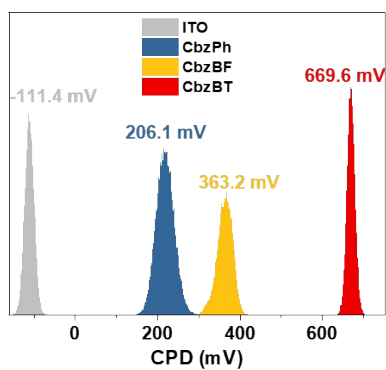


Figure S7. Statistical distribution of CPD extracted from corresponding KPFM images.

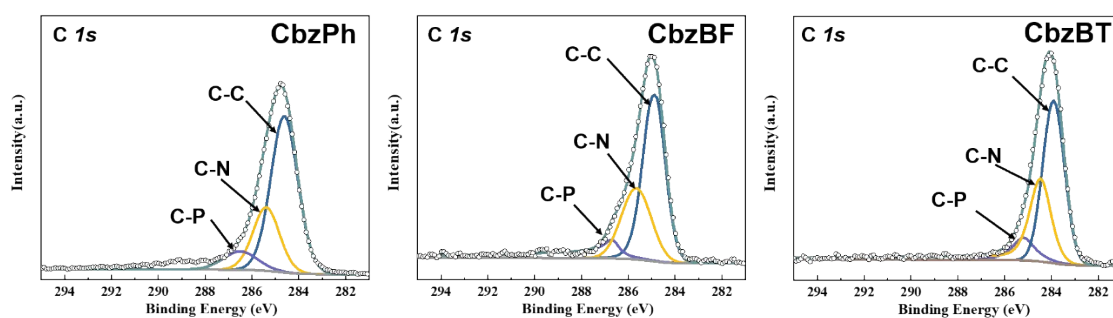


Figure S8. X-ray photoelectron spectra of C1s for CbzPh, CbzBF and CbzBT modified ITO.

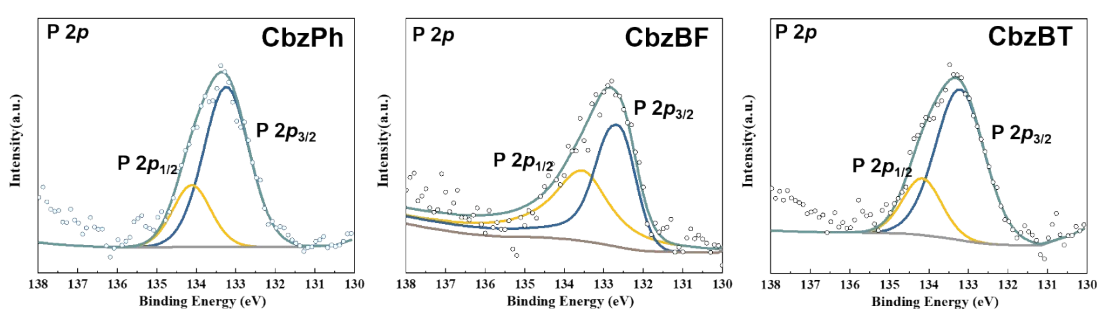


Figure S9. X-ray photoelectron spectra of P 2p for CbzPh, CbzBF and CbzBT modified ITO.

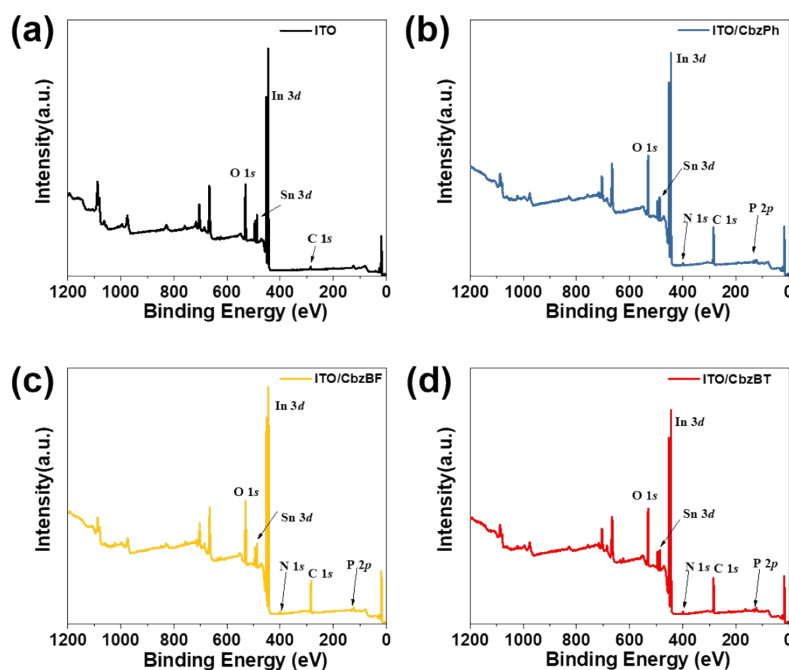


Figure S10. HR-XPS surveys of bare ITO, CbzPh, CbzBF and CbzBT-modified ITO

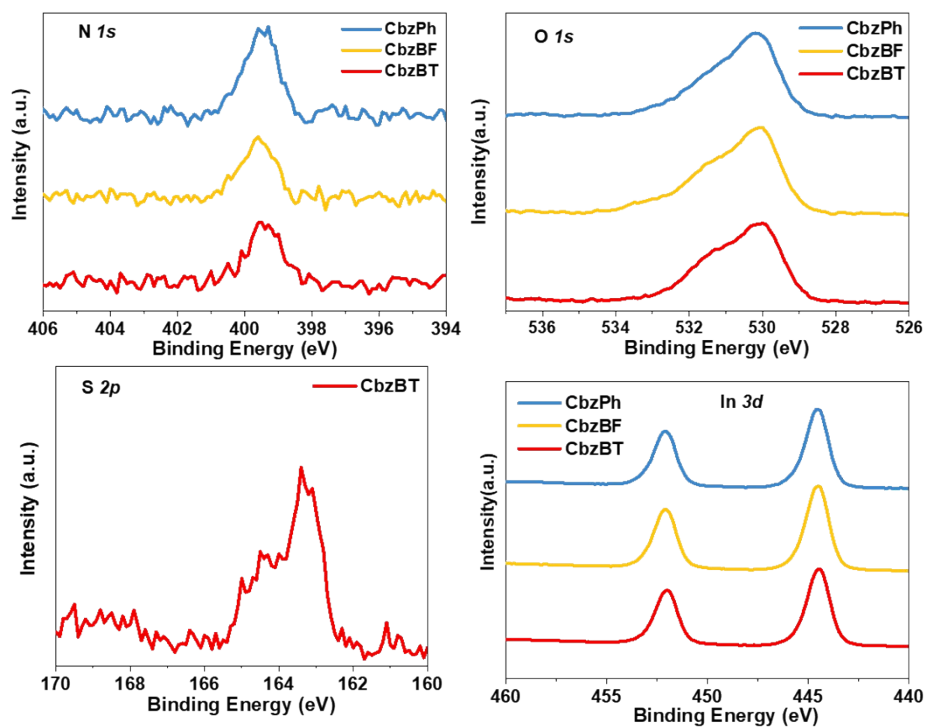


Figure S11. The X-ray photoelectron spectroscopy at the N $1s$, O $1s$, S $2p$ and In $3d$ regions of bare ITO, CbzPh, CbzBF and CbzBT-modified ITO.

Table S3. C $1s$ and In $3d_{3/2}$ core-level peak area as measured by XPS for different SAM on ITO covered glass substrate. The C $1s$ peak area is divided by the number of carbon atoms and a relative coverage factor is calculated by normalizing to the In $3d_{3/2}$ core level area

SAM	C $1s$ Area	In $3d_{3/2}$ Area	# atoms	Carbon Coverage factor
ITO+CbzPh	62205.3	382278.6	20	$8.14 \cdot 10^{-3}$
ITO+CbzBF	68910.6	375012.7	22	$8.35 \cdot 10^{-3}$
ITO+CbzBT	69831.0	367763.4	22	$8.63 \cdot 10^{-3}$

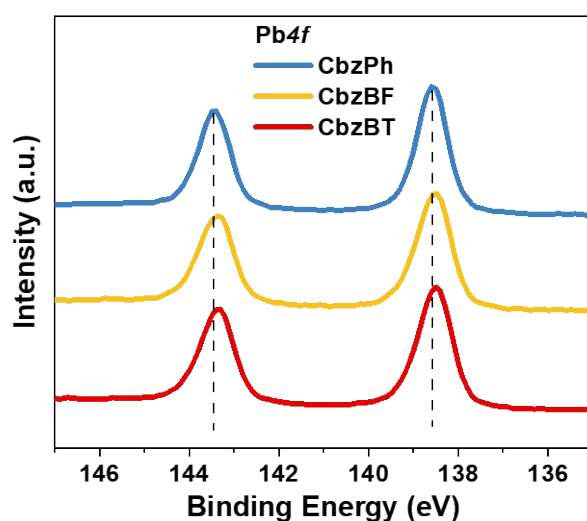


Figure S12. XPS spectra showing the evolution of Pb *4f* core levels of the buried perovskite film peeled off from CbzPh, CbzBF and CbzBT-modified ITO. The buried interface was obtained by exfoliating the perovskite film from the glass/ITO/SnO₂ substrate. The specific method is as follows^[3]: The surface of the perovskite film was coated by UV curable glue and covered with glass, followed by the application of pressure on the glass. The samples were then placed in a UV lamp box (350 W) for 1 min to cure the UV adhesive. Finally, two tweezers were used to clamp the substrate and glass. Then the perovskite film was peeled off from the substrate.



Figure S13. Water contact angles of bare ITO, CbzPh-, CbzBF- and CbBT-modified ITO.

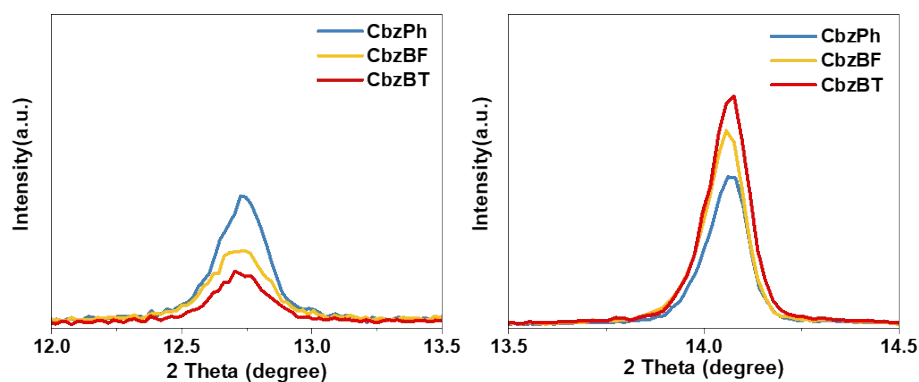


Figure S14. The PbI₂ and (110) peaks of perovskite films deposited on CbzPh-, CbzBF- and CbBT-modified ITO.

7. Device Fabrication and characterization

The pre-patterned ITO-coated glass substrates ($15 \Omega \text{ sq}^{-1}$) were sequentially cleaned by sonication with detergent (Decon 90), deionized (DI) water, acetone, and isopropyl alcohol for 15 min, respectively, and subsequently dried in an oven overnight. The cleaned ITO substrates are treated with UV ozone (Novascan UV-ozone Cleaners) for 30 min right before being transferred into a nitrogen glovebox for device fabrication. SAM solutions are prepared by dissolving CbzPh, CbzBF and CbzBT (1 mM) in IPA and stirred for 30 min at 80 °C before deposition. 40 uL of the SAM solution is dropped onto the substrates and spin-coated at 3000 rpm for 30 s. Then after annealing at 100 °C for 15 min, the substrates are washing with IPA (60 uL) through spin-coating at 3000 rpm for 30 s, then anneal at 100 °C for 5 min.

1.6 M perovskite precursor solution was prepared by mixing FAI, PbI_2 , MAI and CsI in DMF:DMSO mixed solvent (4:1 v:v) with the chemical formula $\text{Cs}_{0.05}\text{MA}_{0.15}\text{FA}_{0.80}\text{PbI}_3$. 15 mol% of MAcl was added to the precursor before deposition. After stirring for over 6 h, the precursor is transferred for spin-coating. 50 uL of the precursor was dripped onto SAM-based substrates and spin-coating at 1000 rpm for 7 s and 5000 rpm for 39 s, 180uL CB as anti-solvent is dripped at the final 20 s. Then the perovskite films were annealed at 100 °C for 30 min. For the surface passivation, PI (0.3 mg/mL in IPA) was spin-coated on perovskite film at 4000 rpm for 30 s, then annealed at 100 °C for 10 min.^[4] The films were transferred to thermal evaporator for deposition of C_{60} , BCP and Ag with a thickness of 25 nm, 6 nm and 100 nm under a high vacuum ($<4 \times 10^{-6}$ torr). For the anti-reflection coating, a MgF_2 layer with a thickness of 110 nm was thermal evaporated onto the backside of devices.

J-V characteristics of PSC devices were measured in nitrogen glovebox at room temperature by using a Keithley 2400 source meter under simulated sunlight from a solar simulator (Enlitech, SS-F5, Taiwan). EQE is measured by an EnLi Technology (Taiwan) EQE measurement system. A National Renewable Energy Laboratory calibrated silicon solar cell is used to calibrate the AM 1.5 G light intensity. The PVCs are equipped with a shading mask with an aperture area of 0.04 cm² to ensure the accuracy of current density in *J-V* curves. The operational stability tests were carried out at the MPP for the unencapsulated cells under AM 1.5 G illumination in N₂ atmosphere which was produced by a xenon-lamp-based solar simulator. The bias at the MPP was calculated and applied automatically. The light intensity was calibrated by a standard silicon reference cell from Newport.

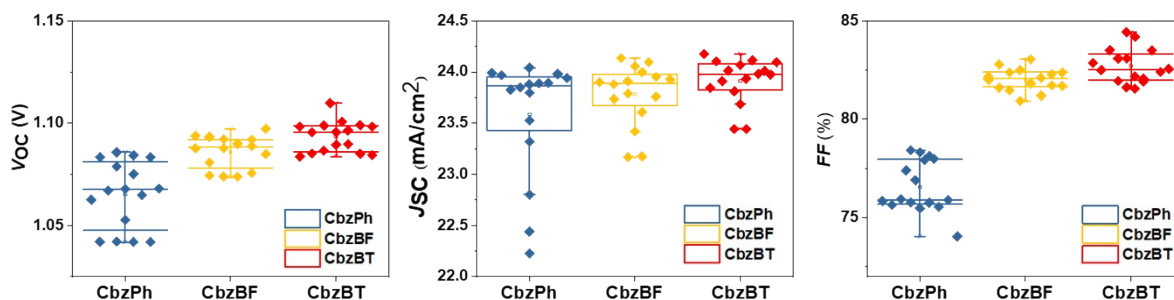


Figure S15. Statistical V_{OC} (a), J_{SC} (b) and FF (c) of the PSCs with SAM-modified substrates of CbzPh, CbzBF and CbzBT.

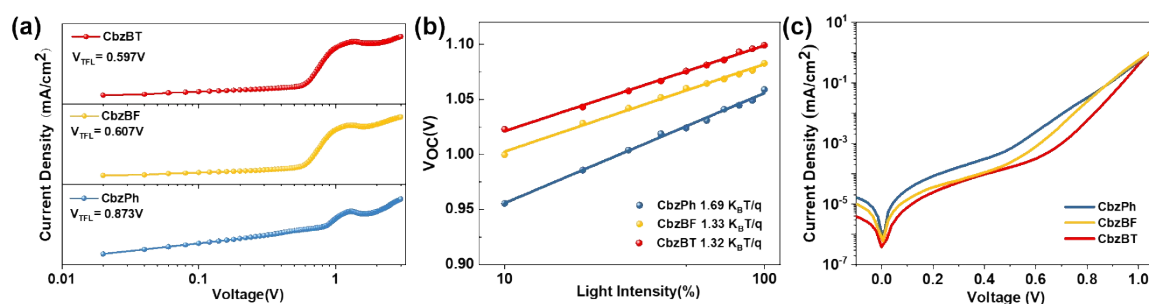


Figure S16. (a) SCLC results of the hole-only devices with CbzPh-, CbzBF- and CbzBT-modified substrates; light intensity-dependent V_{OC} (linearly fitted to obtain the ideality factors) (b) and dark $J-V$ curves (c) of the PSCs with SAM-modified substrates of CbzPh, CbzBF and CbzBT.

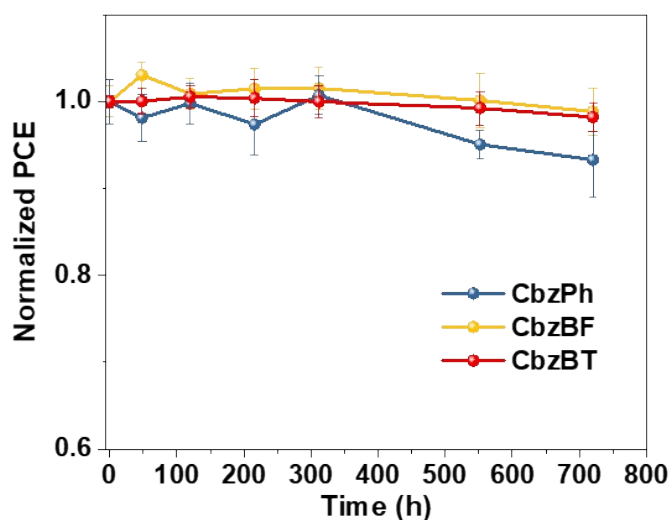


Figure S17. The normalized PCE of unencapsulated PSC devices aged at 65°C in nitrogen atmosphere, the error bar indicates the standard deviation of 15 devices.

Table S4. Lifetimes and weight fractions derived from time-resolved PL decay traces^[a].

Sample	τ_1 [ns]	A_1 [%]	τ_2 [ns]	A_2 [%]	τ_{avg} [ns]
ITO/CbzPh/Pvk	20	0.43	2120	99.57	2120
ITO/CbzBF/Pvk	15	0.13	4346	99.87	4346
ITO/CbzBT/Pvk	20	0.07	5031	99.93	5031

^[a]The TRPL decay curves (Figure S17b) are fitted by bi-exponential decay equation $I(t) = A_1 \exp(-t/\tau_1) + A_2 \exp(-t/\tau_2)$; τ_1 and τ_2 are the lifetimes of fast and slow decays; A_1 and A_2 are the corresponding weight fractions. The average lifetime is calculated using the equation:

$$\tau_{avg} = \frac{\sum_{i=1}^n A_i \tau_i^2}{\sum_{i=1}^n A_i \tau_i}$$

8. ¹H and ¹³C NMR spectra

20230713-CbzBF-C4Br. 1. fid

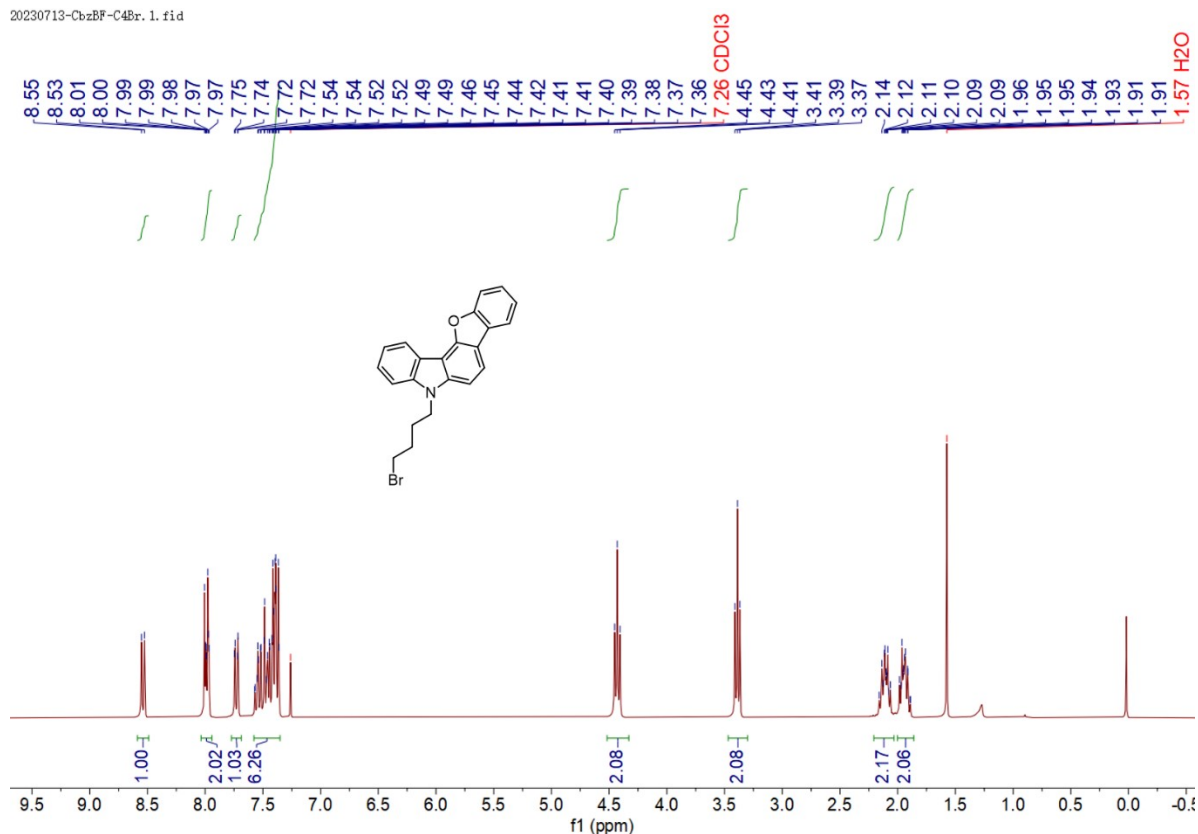


Figure S18. ¹H NMR spectra of 5-(4-bromobutyl)-5H-benzofuro[3,2-c]carbazole in CDCl₃.

20230715-CbzBF-C4Br. 1. fid

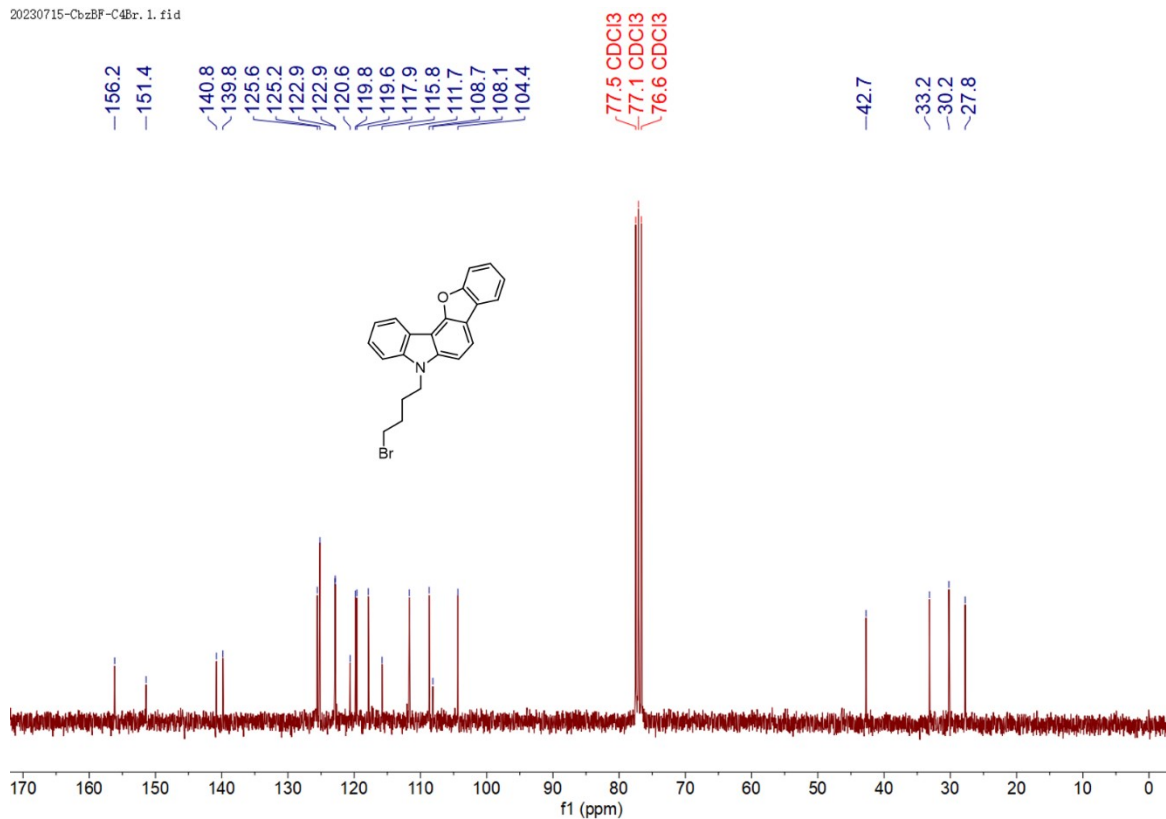


Figure S19. ^{13}C NMR spectra of 5-(4-bromobutyl)-5H-benzofuro[3,2-c]carbazole in CDCl_3 .

20230713-CbzBF-C4PO3Et2. 1. fid

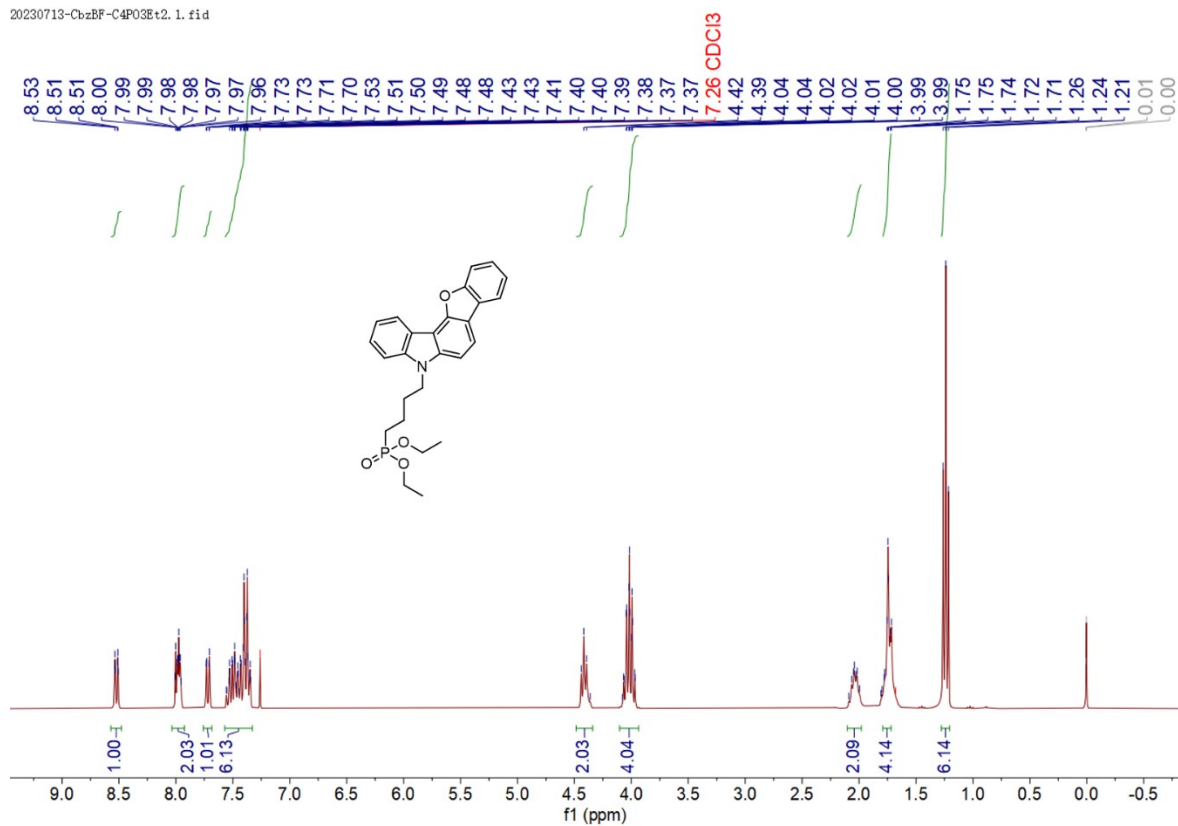


Figure S20. ^1H NMR spectra of diethyl (4-(5H-benzofuro[3,2-c]carbazol-5-yl)butyl)phosphonate in CDCl_3 .

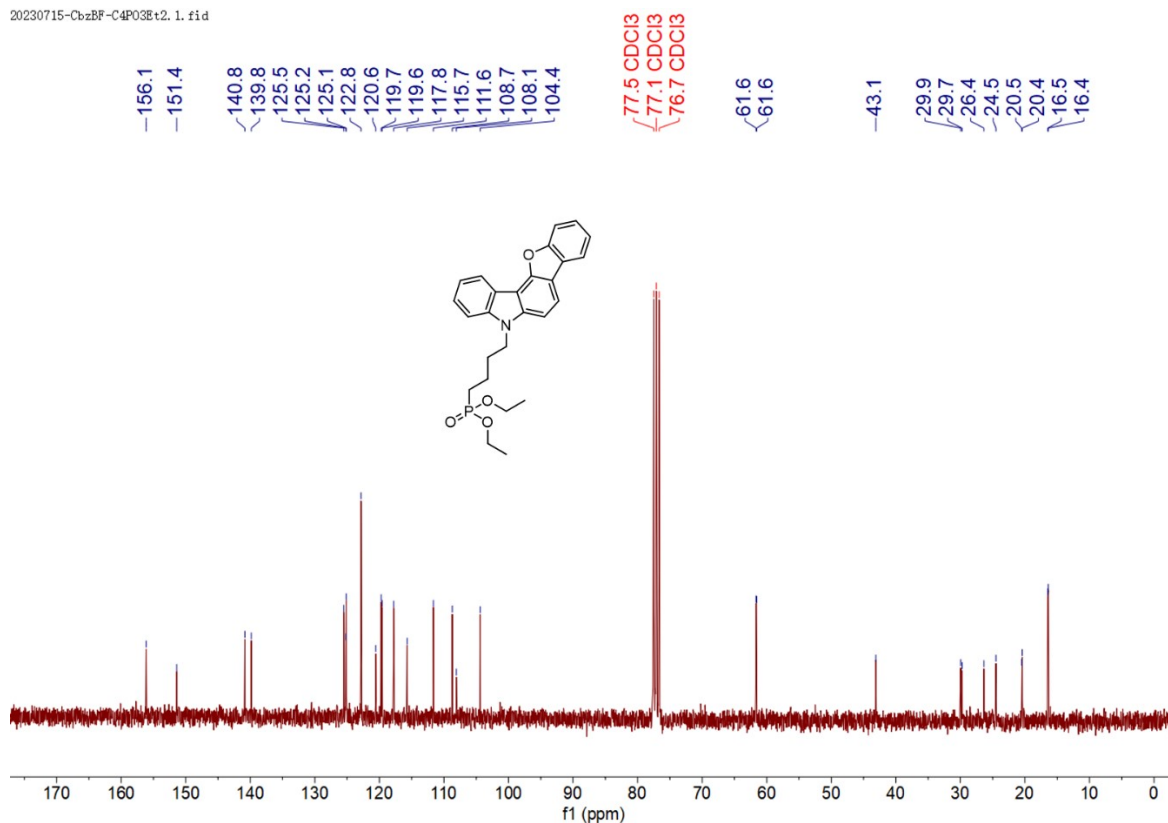


Figure S21. ¹³C NMR spectra of diethyl (4-(5*H*-benzofuro[3,2-*c*]carbazol-5-yl)butyl)phosphonate in CDCl₃.

nmr/BFC4PO3H2

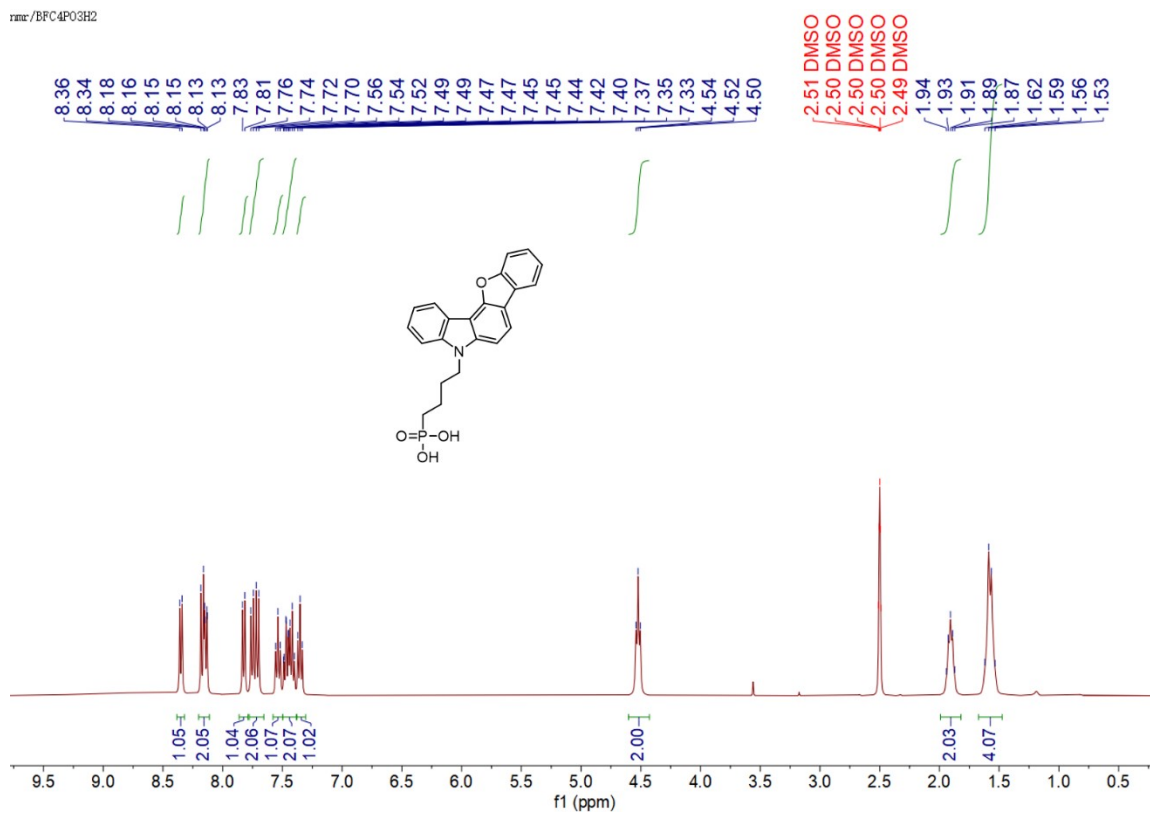


Figure S22. ¹H NMR spectra of (4-(5*H*-benzofuro[3,2-*c*]carbazol-5-yl)butyl)phosphonic acid (CbzBF) in DMSO-*d*₆.

20230823-CbzBF-C4P03H2. 2. fid

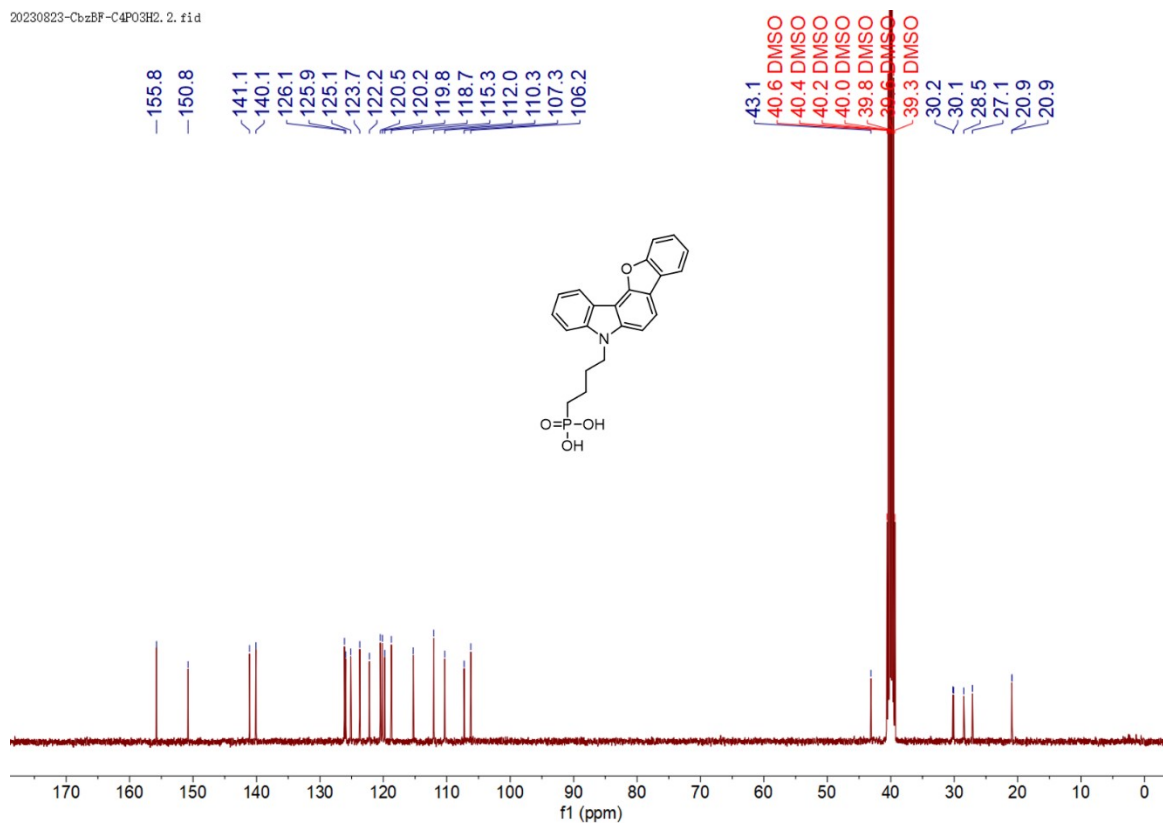


Figure S23. ^{13}C NMR spectra of (4-(5*H*-benzofuro[3,2-*c*]carbazol-5-yl)butyl)phosphonic acid (CbzBF) in $\text{DMSO-}d_6$.

20230422-BTCbz-C4Br. 1. fid

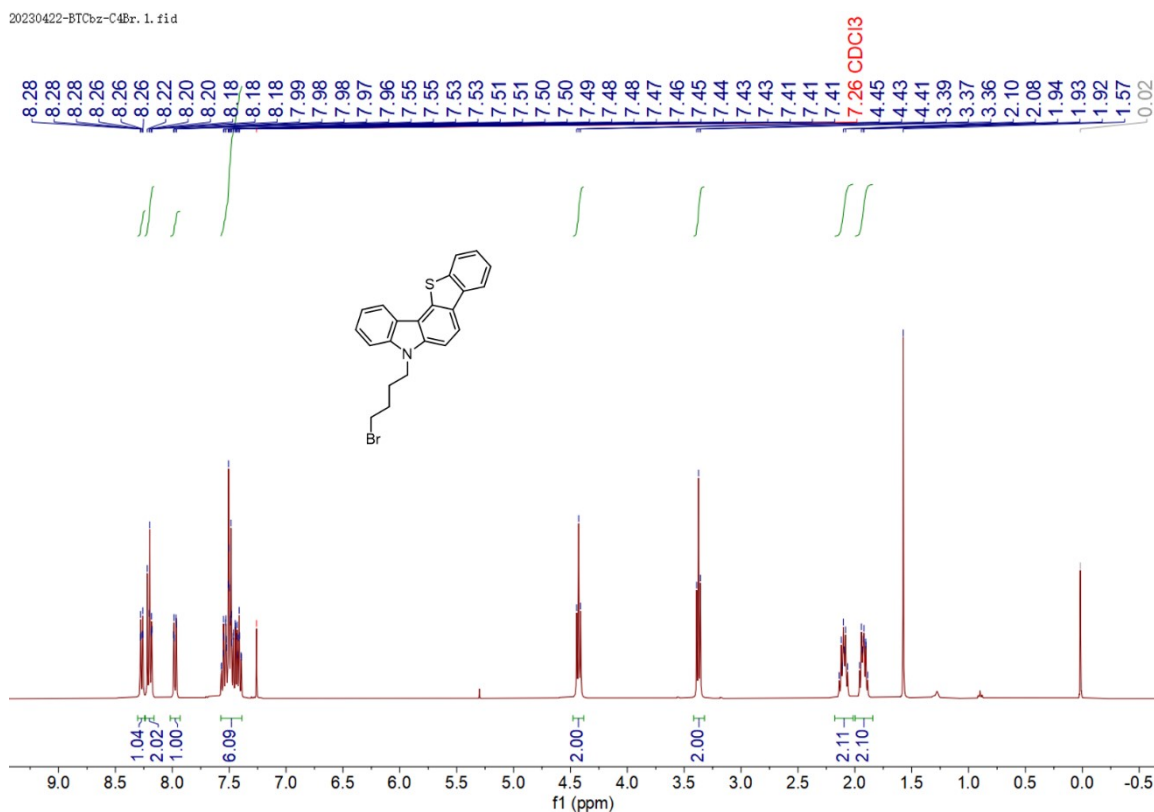


Figure S24. ^1H NMR spectra of diethyl 5-(4-bromobutyl)-5*H*-benzo[4,5]thieno[3,2-*c*]carbazole in CDCl_3 .

20230422-BTCbz-C4Br. 2. fid

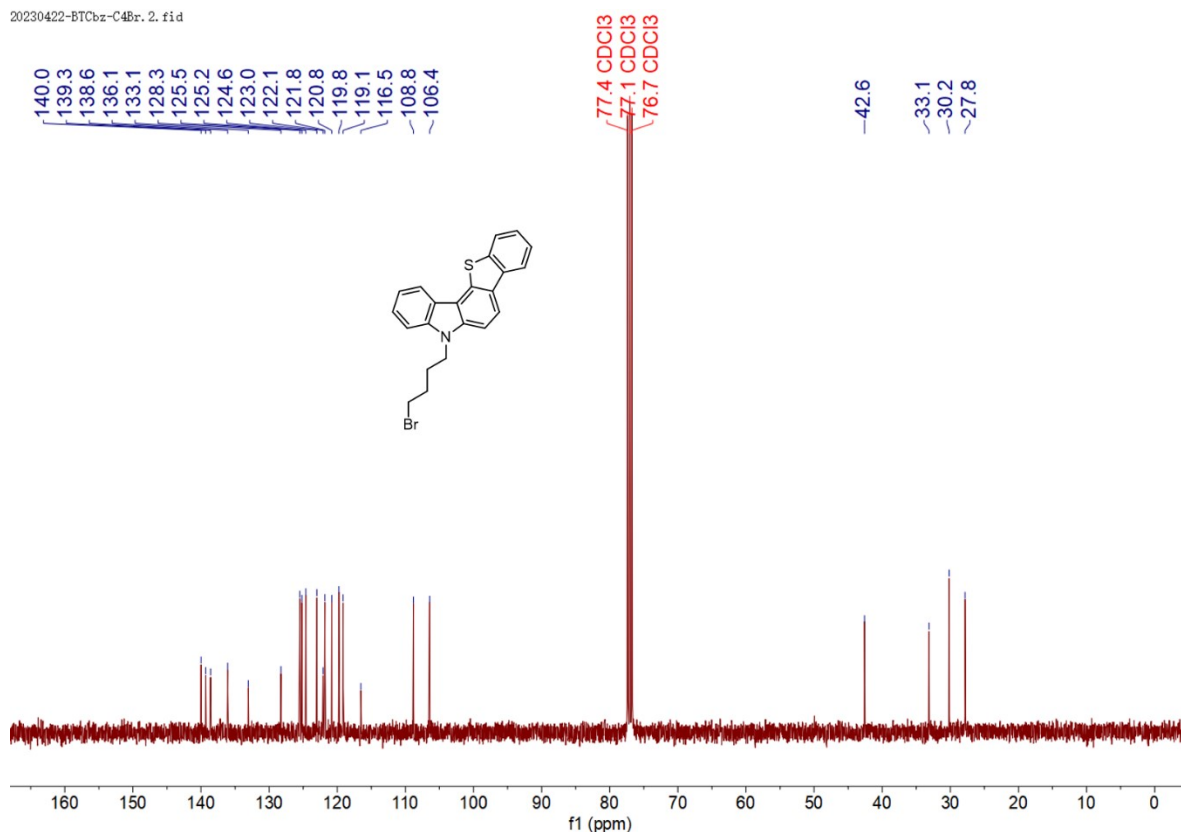


Figure S25. ¹³C NMR spectra of diethyl 5-(4-bromobutyl)-5H-benzo[4,5]thieno[3,2-c]carbazole in CDCl₃.

20230818-CbzBT-C4P03Et2. 2. fid

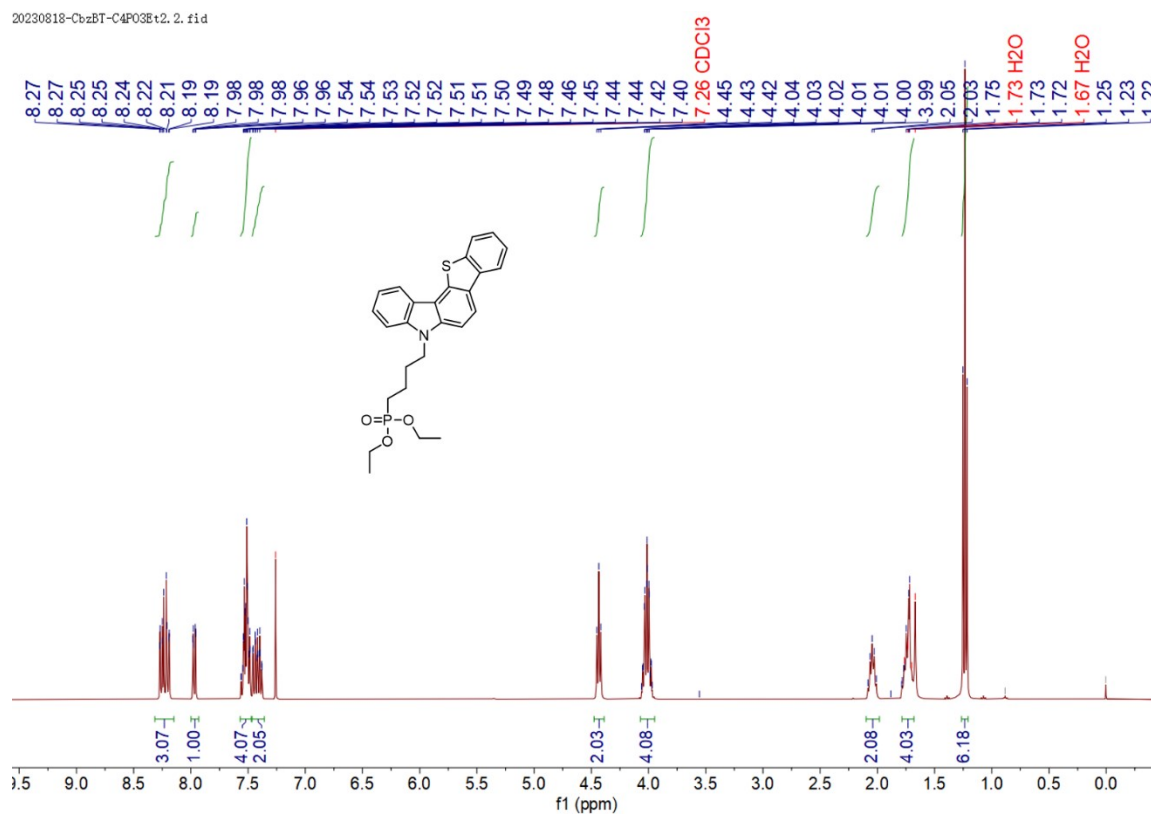


Figure S26. ¹H NMR spectra of diethyl (4-(5H-benzo[4,5]thieno[3,2-c]carbazol-5-yl)butyl)phosphonate in CDCl₃.

20230818-CbzBT-C4P03Et2. 3. fid

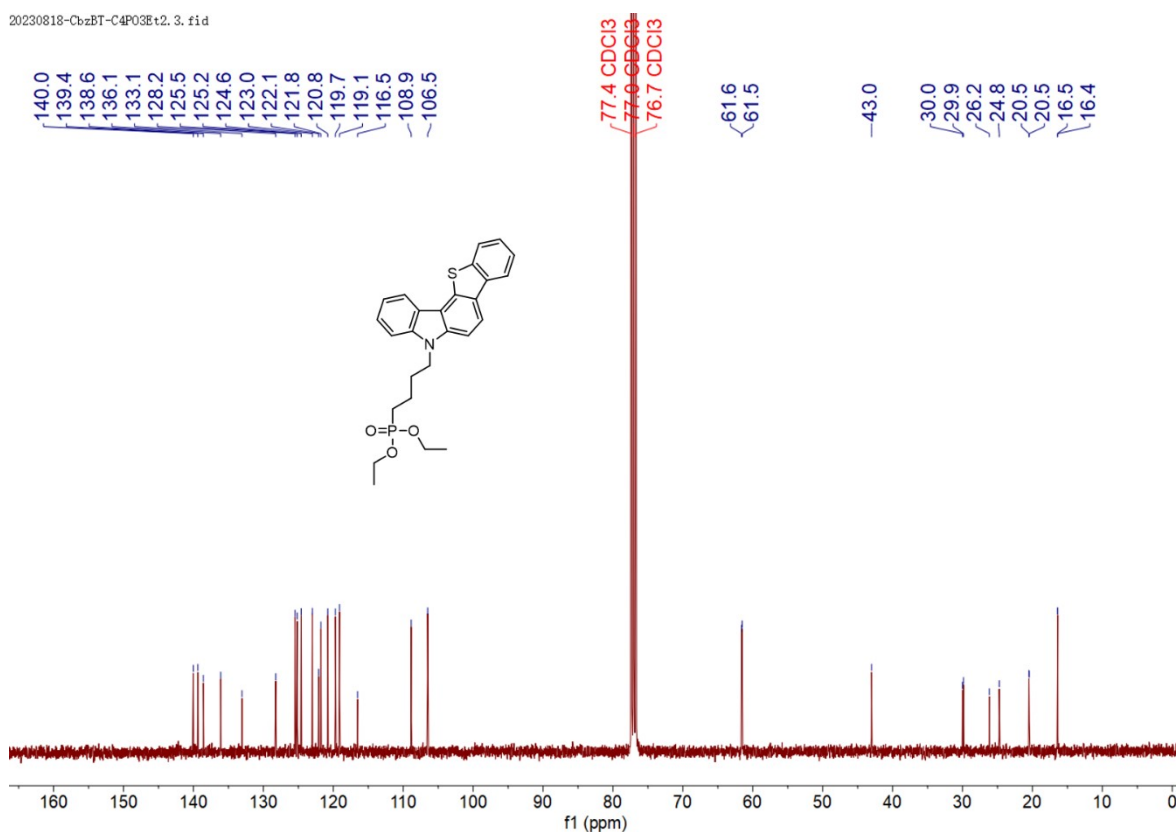


Figure S27. ¹³C NMR spectra of diethyl (4-(5H-benzo[4,5]thieno[3,2-c]carbazol-5-yl)butyl)phosphonate in CDCl₃.

20230823-CbzBT-C4P03H2. 1. fid

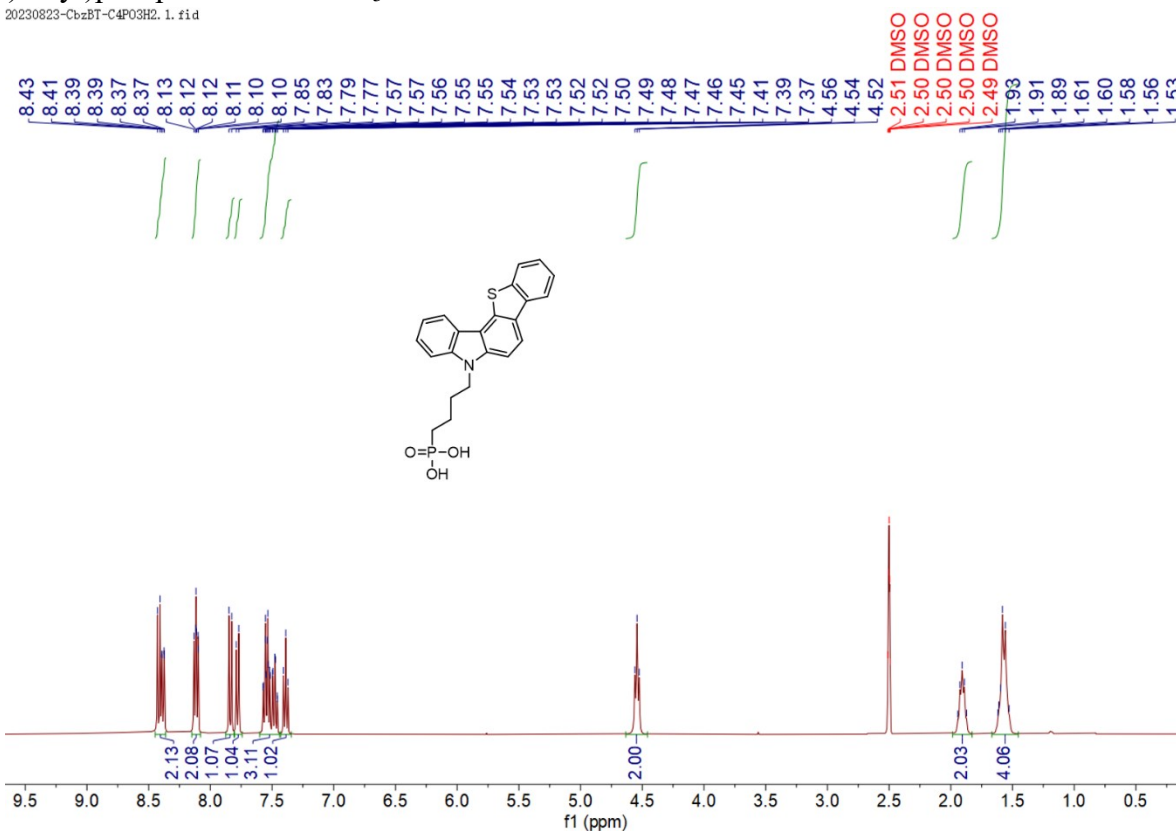


Figure S28. ¹H NMR spectra of (4-(5H-benzo[4,5]thieno[3,2-c]carbazol-5-yl)butyl)phosphonic acid (CbzBT) in DMSO-*d*₆.

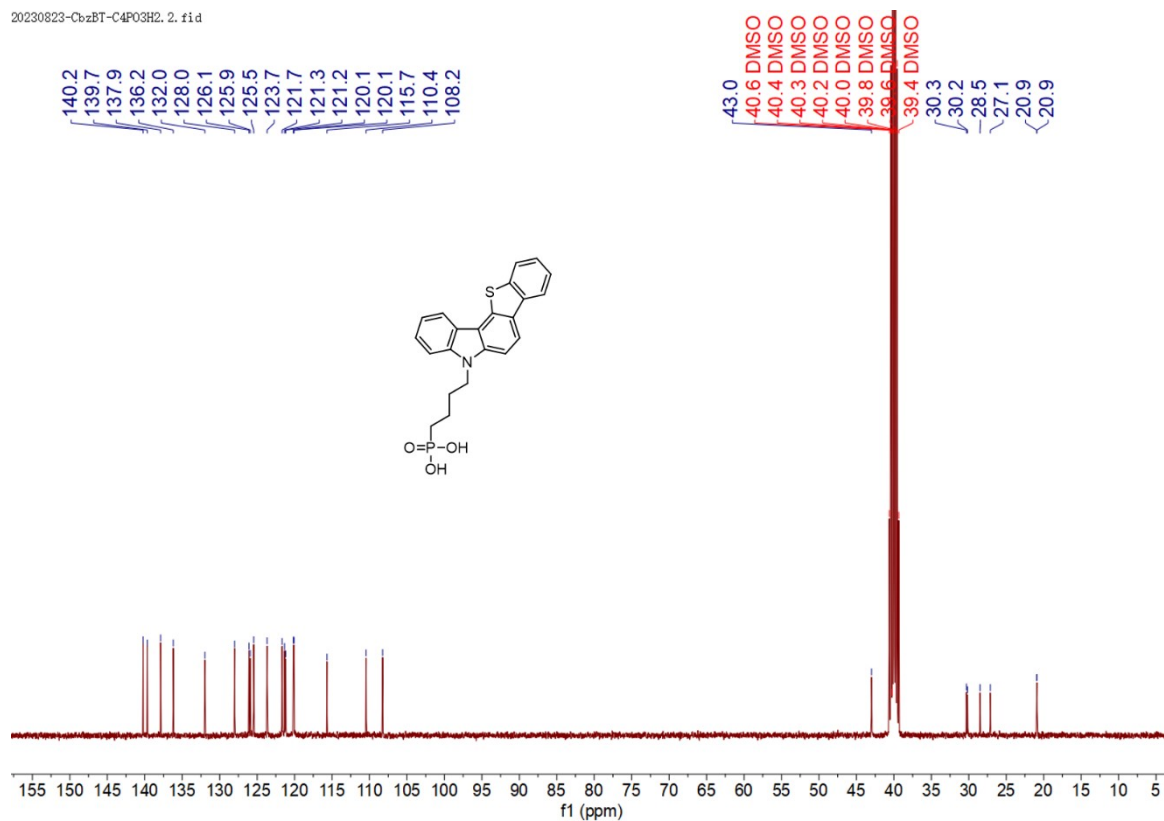


Figure S29. ¹³C NMR spectra of (4-(5H-benzo[4,5]thieno[3,2-c]carbazol-5-yl)butyl)phosphonic acid (CbzBT) in DMSO-*d*₆.

MALDI, J06, 20231206

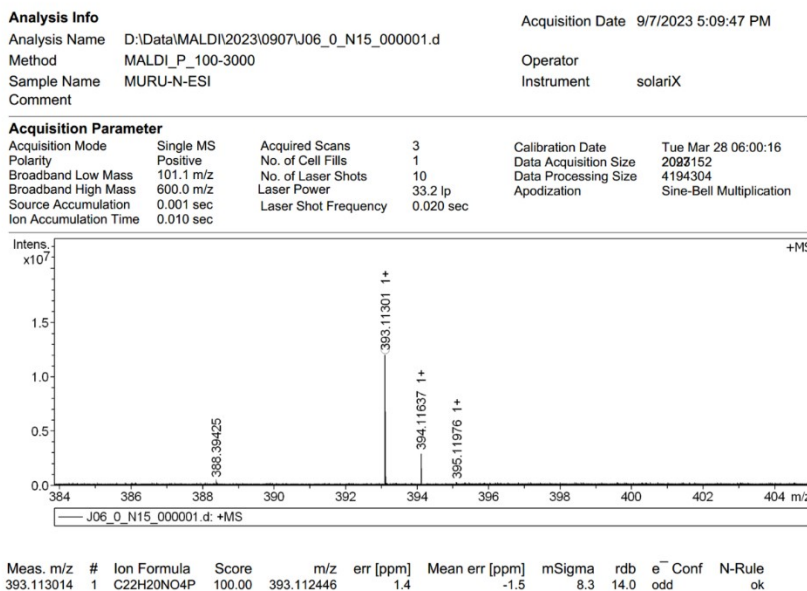


Figure S30. HR-MS (MALDI-TOF) of (4-(5H-benzofuro[3,2-c]carbazol-5-yl)butyl)phosphonic acid (CbzBF).

MALDI, J05, 20231206

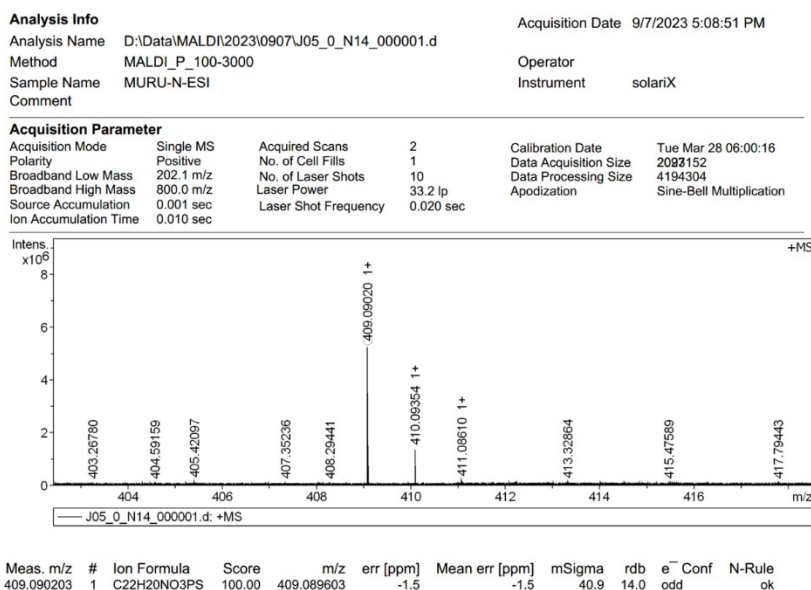


Figure S31. HR-MS (MALDI-TOF) of (4-(5H-benzo[4,5]thieno[3,2-c]carbazol-5-yl)butyl)phosphonic acid (CbzBT).

9. References

- [1] A. Al-Ashouri, E. Kohnen, B. Li, A. Magomedov, H. Hempel, P. Caprioglio, J. A. Marquez, A. B. Morales Vilches, E. Kasparavicius, J. A. Smith, N. Phung, D. Menzel, M. Grischek, L. Kegelmann, D. Skroblin, C. Gollwitzer, T. Malinauskas, M. Jost, G. Matic, B. Rech, R. Schlatmann, M. Topic, L. Korte, A. Abate, B. Stannowski, D. Neher, M. Stolterfoht, T. Unold, V. Getautis, S. Albrecht, *Science* **2020**, *370*, 1300-1309.
- [2] M. J. Frisch, G. W. Trucks, H. B. Schlegel, G. E. Scuseria, M. A. Robb, J. R. Cheeseman, G. Scalmani, V. Barone, B. Mennucci, G. A. Petersson, H. Nakatsuji, M. Caricato, X. Li, H. P. Hratchian, A. F. Izmaylov, J. Bloino, G. Zheng, J. L. Sonnenberg, M. Hada, M. Ehara, K. Toyota, R. Fukuda, J. Hasegawa, M. Ishida, T. Nakajima, Y. Honda, O. Kitao, H. Nakai, T. Vreven, J. A. Montgomery, J. E. Peralta, F. Ogliaro, M. Bearpark, J. J. Heyd, E. Brothers, K. N. Kudin, V. N. Staroverov, R. Kobayashi, J. Normand, K. Raghavachari, A. Rendell, J. C. Burant, S. S. Iyengar, J. Tomasi, M. Cossi, N. Rega, J. M. Millam, M. Klene, J. E. Knox, J. B. Cross, V. Bakken, C. Adamo, J. Jaramillo, R. Gomperts, R. E. Stratmann, O. Yazyev, A. J. Austin, R. Cammi, C. Pomelli, J. W. Ochterski, R. L. Martin, K. Morokuma, V. G. Zakrzewski, G. A. Voth, P. Salvador, J. J. Dannenberg, S. Dapprich, A. D. Daniels, O. Farkas, J. B. Foresman, J. V. Ortiz, J. Cioslowski, D. J. Fox, Gaussian 09, gaussian, Inc., Wallingford CT, **2009**.
- [3] S. Chen, X. Dai, S. Xu, H. Jiao, L. Zhao, J. Huang, *Science* **2021**, *373*, 902-907.
- [4] a) F. Li, X. Deng, F. Qi, Z. Li, D. Liu, D. Shen, M. Qin, S. Wu, F. Lin, S. H. Jang, J. Zhang, X. Lu, D. Lei, C. S. Lee, Z. Zhu, A. K. Jen, *J Am Chem Soc* **2020**, *142*, 20134-20142; b) X. Deng, F. Qi, F. Li, S. Wu, F. R. Lin, Z. Zhang, Z. Guan, Z. Yang, C. S. Lee, A. K. Jen, *Angew Chem Int Ed Engl* **2022**, *61*, e202203088; c) W. Jiang, F. Li, M. Li, F. Qi, F.

R. Lin, A. K. Jen, *Angew Chem Int Ed Engl* **2022**, *61*, e202213560; d) M. Liu, L. Bi, W. Jiang, Z. Zeng, S. W. Tsang, F. R. Lin, A. K. Jen, *Adv Mater* **2023**, e2304415.